



## OPEN The regulatory role of *ACP5* in the diesel exhaust particle-induced AHR inflammatory signaling pathway in a human bronchial epithelial cell line

Aaron Yu<sup>1,10</sup>, Dankyu Yoon<sup>2,10</sup>, Hye Bin An<sup>1,10</sup>, Uimook Choi<sup>3</sup>, Hye-Ryeon Heo<sup>2</sup>, Dong-Hoon Chae<sup>1</sup>, Hyun Sung Park<sup>1</sup>, Jae Han Park<sup>1</sup>, Myoung Hee Han<sup>1</sup>, Jiyoung Heo<sup>1</sup>, Keonwoo Cho<sup>1</sup>, Ki-Sun Park<sup>4</sup>, Hee Min Yoo<sup>5,6</sup>, Hyung-Sik Kim<sup>7,8</sup>, Kyung-Sun Kang<sup>9</sup>, Mi-Kyung Oh<sup>1</sup>, Hyun Joung Lim<sup>2</sup> & Kyung-Rok Yu<sup>1</sup>✉

Exposure to diesel exhaust particles (DEPs), which are major constituents of urban air pollution, is associated with adverse health outcomes. Previous studies have shown that DEPs enhance the expression of pro-inflammatory cytokines and immune responses. However, few studies have focused on genomic variants that regulate DEP-induced signaling. Here, we identify a frequently found genomic variant, *ACP5*, in allergic diseases, and establish an *ACP5* knock-out (KO) human bronchial epithelial cell line (BEAS-2B) using CRISPR/Cas9 editing to mimic the *ACP5* mutation. DEP-induced apoptosis and intracellular reactive oxygen species (ROS) were significantly increased in the *ACP5* KO cells compared with controls, suggesting that *ACP5* KO cells were at increased risk from DEP exposure. A gene expression profile revealed an activated aryl hydrocarbon receptor (AHR)-CYP1A1 axis followed by upregulated pro-inflammatory signaling. Treatment of a DEP-exposed *ACP5* KO BEAS-2B conditioned medium (CM) supernatant induced an inflammatory response and tissue damage in mice, and AHR inhibition effectively prevented inflammation-induced damage, suggesting that AHR-CYP1A1-inflammatory signaling is a prominent mechanism responsible for detrimental effects. Collectively, our findings reveal a novel link between *ACP5* KO and the AHR-CYP1A1 inflammatory signaling pathway in DEP-exposed cells, and identify the AHR-CYP1A1 axis as a potential therapeutic target in individuals suffering from DEP-induced toxicity, particularly those with *ACP5* mutations.

**Keywords** *ACP5*, Diesel exhaust particles, BEAS-2B, Aryl hydrocarbon receptor, Inflammatory response

### Abbreviations

ACP5	Acid phosphatase 5
AD	Atopic dermatitis
AHR	Aryl hydrocarbon receptor
ALT	Alanine amino transferase
AR	Allergic rhinitis

<sup>1</sup>Department of Agricultural Biotechnology and Research Institute of Agriculture and Life Sciences, Seoul National University, Seoul 08826, Korea. <sup>2</sup>Division of Cardiovascular Disease Research, Department of Chronic Disease Convergence, Korea National Institute of Health, Cheongju 28159, Korea. <sup>3</sup>Laboratory of Clinical Immunology and Microbiology, NIAID, NIH, North Bethesda, USA. <sup>4</sup>KM Science Research Division, Korea Institute of Oriental Medicine, Daejeon 34054, Korea. <sup>5</sup>Biometrology Group, Korea Research Institute of Standards and Science (KRISS), Daejeon 34113, Korea. <sup>6</sup>Department of Bio-Analytical Science, University of Science and Technology (UST), Daejeon 34113, Korea. <sup>7</sup>Department of Life Science in Dentistry, School of Dentistry, Pusan National University, Yangsan 50612, Korea. <sup>8</sup>Dental and Life Science Institute, Pusan National University, Yangsan 50612, Korea. <sup>9</sup>Adult Stem Cell Research Center and Research, Institute for Veterinary Science, College of Veterinary Medicine, Seoul National University, Seoul 08826, Korea. <sup>10</sup>Aaron Yu, Dankyu Yoon and Hye Bin An contributed equally to this work. ✉email: cellyu@snu.ac.kr

ARNT	Aryl hydrocarbon receptor nuclear translocator
AS	Asthma
AST	Aspartate amino transferase
BEAS-2B	Human bronchial epithelial cell line
CM	Conditioned media
CYP1A1	Cytochrome P4501A1
DCFDA	2',7'-dichlorofluorescein diacetate
DEP	Diesel exhaust particles
FBAT	Family-based association test
GWAS	Genome-wide association studies
IPA	Ingenuity pathway analysis
NAC	N-acetyl-L-cysteine
PAHS	Polycyclic aromatic hydrocarbons
ROS	Reactive oxygen species
TRAP	Tartrate-resistant acid phosphatase
XRE	Xenobiotic responsive element

Air pollution is a major global health concern as industrialization and expansion of urban environments continue. Exposure to air pollutants is unavoidable and is now top-10 risk factor for all-cause death worldwide. Air pollution consists of a mixture of gases, volatile organic compounds, and particulate matter (PM). PM is categorized as coarse (<10  $\mu\text{m}$  in diameter), fine (<2.5  $\mu\text{m}$ ), or ultrafine (<0.2  $\mu\text{m}$ ). The presence of fine and ultrafine PM is correlated with mortality as smaller particles can penetrate deep into the lungs and circulate within the body<sup>1</sup>. Diesel exhaust particles (DEPs) constitute up a significant proportion of urban fine and ultrafine PM, and the health effects of DEPs have been studied intensively.

DEPs comprise complex mixtures of organic and inorganic compounds, including polycyclic aromatic hydrocarbons (PAHs). Because of their fine-to-ultrafine size, PAHs are readily deposited in and penetrate the gas-exchange regions of the lung<sup>2</sup>. PAH toxicity is linked to the formation of reactive metabolites and activation of cellular receptors, and the aryl hydrocarbon receptor (AHR) in particular<sup>3</sup>.

The AHR signaling pathway is found in wide range of species, tissues, and cell types. Constitutive AHR expression is significantly high in first-line defense organs such as the skin, lung, liver, and gut<sup>4</sup>. Activated AHR signals induce a specific DNA recognition sequence, GCGTG, within a responsive element known as the xenobiotic responsive element (XRE). Because XREs are in the promoter regions of a number of receptor-regulated genes, differential alteration of gene expression, such as the induction of cytochrome P4501A1 (CYP1A1), occurs upon AHR activation. The generation of ROS and the resulting oxidative stress has also been identified as a major mechanism responsible for the effects of DEP-induced AHR signaling<sup>5</sup>.

Oxidative stress caused by PAH-induced ROS generation triggers activation of alveolar macrophages and bronchial epithelia cells in response to the pro-inflammatory phenotype (M1 macrophages) and the release of pro-inflammatory cytokines<sup>6</sup>. As exposure to DEP increases the susceptibility of the lungs to infection<sup>6</sup>, we hypothesized that a genetic variant may be associated with risks from and susceptibility to disease, particularly when exposed to DEP.

Tartrate-resistant acid phosphatase (TRAP/ACP5) is a class of metalloenzymes that catalyze the hydrolysis of various phosphate esters and anhydrides in acidic conditions<sup>7</sup>. Macrophages from *ACP5*-null mice showed significantly elevated secretion of pro-inflammatory cytokines such as tumor necrosis factor- $\alpha$  (TNF- $\alpha$ ), interleukin (IL)-1- $\beta$ , and IL-12 when stimulated with a lipopolysaccharide<sup>8</sup>. In immuno-osseous dysplasia spondyloenchondrodysplasia patients with *ACP5*-null or missense mutations, elevation of serum interferon- $\alpha$  activity was detected and gene expression profiling in whole blood defined a type I interferon signature<sup>9</sup>, highlighting the role of ACP5 deficiency in the genesis of autoimmunity.

We designed a post-genome-wide association study of single nucleotide polymorphisms (SNPs) in *ACP5* and susceptibility to DEP. To study the regulatory role of ACP5 on DEP-induced ROS stress in a human bronchial epithelial cell line, BEAS-2B, we knocked out *ACP5* using CRISPR/Cas-9 editing and identified the effects of DEP exposure on the physiological properties of *ACP5* KO BEAS-2B cells. Our findings reveal a previously unrecognized link between ACP5 deficiency and the AHR signaling pathway. This emphasizes the fortified negative effects of DEP exposure on *ACP5*-null cells and downstream signaling.

## Materials and methods

### Study subjects and family-based association analysis

We performed a family-based association study to identify the functional variants responsible for allergy-related diseases in the Korean population. A total of 215 trios (two parents and an affected offspring) were recruited at the Childhood Asthma Atopy Center of the Asan Medical Center. Diseases including allergic disease, asthma, atopic dermatitis, and allergic rhinitis were diagnosed by physicians. The 215 trios were genotyped using Infinium Human Exome BeadChip v1.1 containing approximately 242,000 variants. Demographic features of the study population are listed in Fig. 1A. A total of 47,091 SNPs remained after quality control excluded excessive Mendel errors and monomorphic variants. Of these, 30,220 variants were nonsynonymous. We performed a family-based association analysis on 215 trios with 30,220 nonsynonymous variants using FBAT software<sup>10</sup>. A regional association plot was generated using LocusZoom<sup>11</sup>. This study and the use of all clinical data are approved by the Institutional Review Board (IRB) of Korea Centers for Disease Control and Prevention, where all participants provided written informed consent (IRB No. 2015-07-EXP-01-R-A). All methods are applied in accordance with the relevant guidelines and regulations.

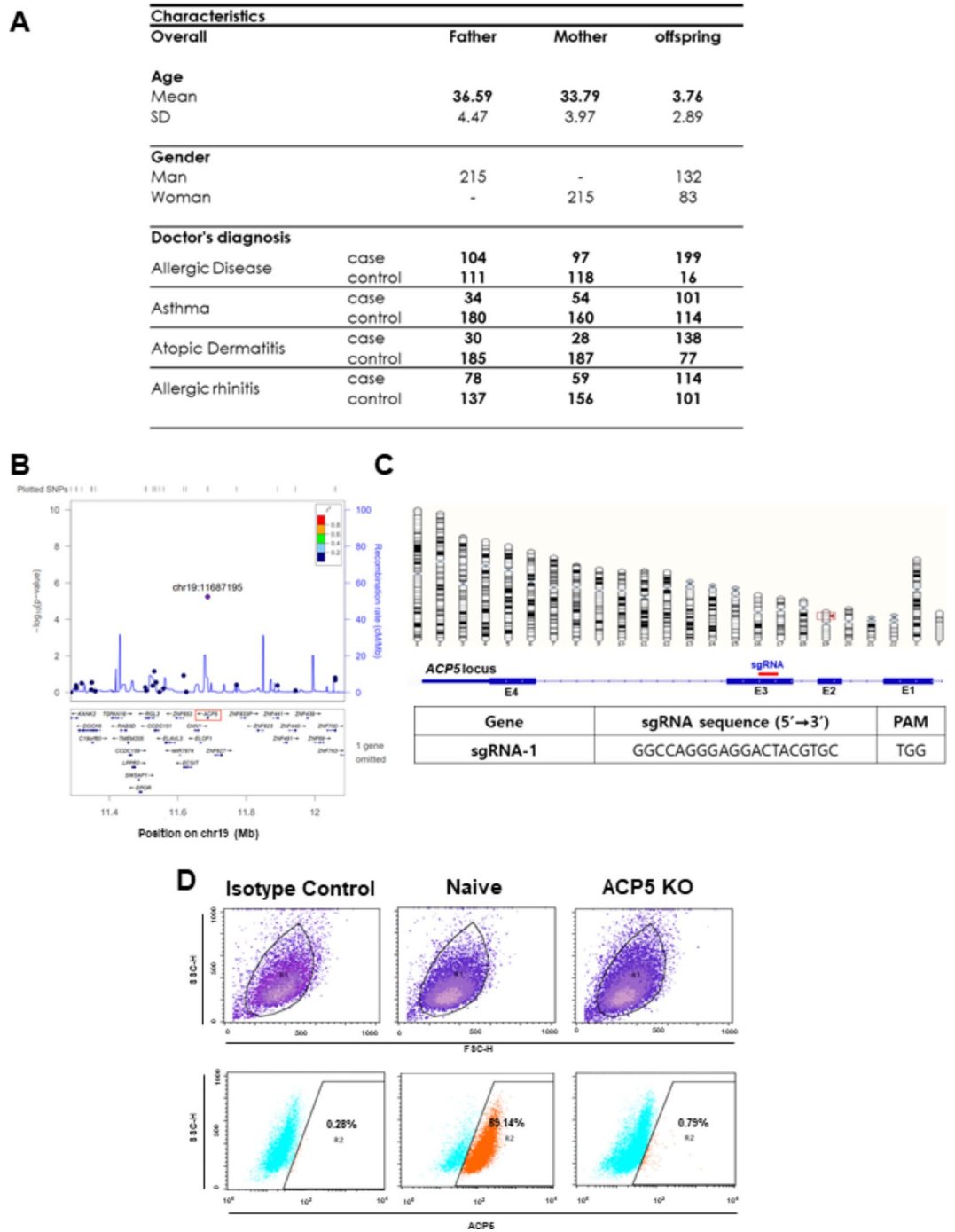


**Fig. 1.** Selection of *ACP5* as a frequent mutation in allergic diseases and establishment of *ACP5* KO BEAS-2B. **(A)** Demographic features of the study population. **(B)** Regional association plots of the chr19:11687195 locus. Genome-wide association studies were conducted to identify associated variants and visualized as a regional map to show their genomic positions and strength of association. **(C)** Chromosomal location of the *ACP5* gene, its exon structure, and SNP. **(D)** Validation of *ACP5* protein expression by flow cytometry analysis.

#### Diesel exhaust particle preparation

Standard Reference Material 1650b diesel PM was obtained from the National Institute of Standards and Technology Gaithersburg, MD, USA. The DEPs were suspended in dimethyl sulfoxide as a 10 mg/mL stock solution.

### BEAS-2B cells preparation and culture

BEAS-2B cells were purchased from ATCC and cultured in Iscove's modified Dulbecco's medium (IMDM; Gibco) supplemented with 10% fetal bovine serum (FBS, Biowest, US origin, premium), 1% antibiotic/antimycotic solution (Gibco) in a humidified atmosphere containing 5% CO<sub>2</sub> at 37 °C. Cells were passaged every 3 or 4 days using 0.05% trypsin/EDTA. The cells were pretreated with 10 mM NAC (Sigma-Aldrich) or 0.75 μM AHR inhibitor, BAY-218 (Selleckchem) before stimulation with DEP (50 μg/mL) as indicated.

### Apoptosis assay

For apoptosis assessment, BEAS-2B cells were seeded into a 12-well plate at 1 × 10<sup>5</sup> cells per well with DEP (0–100 μg/mL) for 24 h. The cells were stained with Annexin-V-FITC (BD Biosciences, Franklin Lakes, NJ, USA) and 7-AAD (BD Biosciences) following the manufacturer's instructions and analyzed by flow cytometry. Reagents and resources used in this study are listed in Table 1.

### Detection of intracellular reactive oxygen species

Intracellular ROS were detected using DCFDA (Sigma-Aldrich). BEAS-2B cells were incubated with various concentrations of DEP for 6 h. After incubation, cells were washed with PBS and incubated with 10 μM DCFDA in a serum-free culture medium for 30 min at 37 °C. The mean DCFDA fluorescence was analyzed using flow cytometer.

### Quantitative real-time PCR

Total RNA was extracted using TRIzol reagent (Invitrogen), and 1 μg of total RNA was converted to cDNA using M-MLV reverse transcriptase (Promega). Real-time PCR was performed using SYBR Green PreMix (enzymatics) and measured using a CFX96 real-time PCR detection system (Biorad). *GAPDH* was used as the reference gene for normalization. The primer sequences for quantitative real-time PCR are listed in Table 2.

### RNA isolation and sequencing

RNA-seq was performed in Macrogen Co. using Illumina technology as previously described, with modifications<sup>12</sup>. Total RNA was extracted using TRIzol reagent (Invitrogen) in *ACP5* KO BEAS-2B cells treated with or without of DEP at a concentration of 50 μg/mL. The mRNA sequencing library was generated using the Illumina Truseq strand mRNA sample preparation kit (Illumina, San Diego, CA, USA) and sequenced using HiSeq2500 (2 × 150 paired-end sequencing, Illumina) according to the manufacturer's protocol. For differential expression analysis, the gene expression of each group was quantified using HISAT2 by mapping the readings to the human gene annotation database (hg38). Next, the differentially expressed genes in *ACP5* KO BEAS-2B cells with or without DEP exposure were shown based on an absolute log<sub>2</sub>-fold change ≥ 0.58 and *p* < 0.01. Heatmaps were then generated and clustering analysis was performed using a hierarchical clustering method.

### Gene ontology analysis and ingenuity pathway analysis

We identified a set of genes based on gene ontology according to three categories: molecular function, biological process, and pathway. The significance of the gene sets (*CYP1A1* [GSE175878], *FOS* [GSE167402], and *NLRP3* [GSE169533]) were calculated using IPA version 2.0 software (Ingenuity Systems, Redwood City, CA). The significance of each factor was calculated using Fisher's exact test.

### BEAS-2B CM collection

BEAS-2B cells were cultured at a concentration of 1.5 × 10<sup>6</sup> cells/150 mm dish for approximately 48 h in IMDM supplemented with 10% FBS, 1% antibiotic/antimycotic solution at 37 °C in 5% CO<sub>2</sub>. At 70–80 confluency, the cells were pretreated with 0.75 μM BAY-218 and cultured with DEP (50 μg/mL) in IMDM for 48 h. The supernatant of the BEAS-2B cell culture was collected and centrifuged at 300 *g* for 10 min and 2500 *g* for 25 min. After centrifugation, the supernatant was concentrated (to approximately 100-fold) by applied pressure using a concentrator (Amicon, Millipore Corporations) with 3000-Da pore-size membranes.

### Animals

All animal experiments and procedures were carried out in accordance with relevant guidelines and regulations approved by the Institutional Animal Care and Use Committee of Seoul National University (protocol no. SNU-221012-3). Additionally, this study is reported in accordance with ARRIVE guidelines. Male C57BL/6 mice were purchased from DBL Co., Ltd. (Seoul, Korea) at 7 weeks of age (Fig. 5).

Figure 4: (1) PBS control, (2) negative control, (3) DEP-treated naïve BEAS-2B cells, (4) NAC pretreated naïve BEAS-2B cells, (5) DEP-treated *ACP5* KO BEAS-2B cells, (6) 0.75 μM BAY-218 pretreated and DEP-treated *ACP5* KO BEAS-2B cells. Mice were injected intraperitoneally with PBS or CM (200 μL) on days 1, 2, 7, and 8.

Figure 5: (1) IMDM media, (2) naïve BEAS-2B cells, (3) DEP-treated naïve BEAS-2B cells, (4) *ACP5* KO BEAS-2B cells. (5) DEP-treated *ACP5* KO BEAS-2B cells, (6) 0.75 μM BAY-218 pretreated DEP-treated *ACP5* KO BEAS-2B cells cultured supernatant (100-fold concentrated). Mice were injected intraperitoneally with PBS or CM (200 μL) on days 1, 2, 7, and 8.

### Biochemical analysis

After animals were euthanized with CO<sub>2</sub> gas on day 10, blood samples were taken and the liver and lungs were removed for analysis. The blood samples were immediately centrifuged at 2,500 rpm 30 min at 25 °C and serum samples were stored at – 80 °C until use. Serum biochemistry of AST and ALT was measured using a Fuji Dri-chem 3500s.

Name	Vendor (Cat#)
FITC Annexin V	BD Biosciences (#556420)
7-AAD (7-Amino-Actinomycin D)	BD Biosciences (#559925)
N-acetyl-L-cysteine (NAC)	Sigma-Aldrich (#A7250)
AHR inhibitor (BAY-218)	Selleckchem (#S8842)

**Table 1.** Reagents and resources.

Gene	Forward primers (5'-3')	Reverse primers (5'-3')
<i>ACP5</i>	ACACTCTTTCCTACACGAGCTCTCCGATCTTGGCTACAGGAGACCT TTGAGGACG	GACTGGAGTTCAGACGTGTGCTC TTCCGATCTTTGGCAATTC GAA GATATTATCTGG
<i>AHR</i>	GTCGTCTAAGGTGTCTGCTGGA	CGCAAACAAAGCCAAGTCTGAGGTG
<i>CYP1A1</i>	GATTGAGCACTGTCAGGAGAAGC	ATGAGGCTCCAGGAGATAGCAG
<i>INF-γ</i>	TCAGCTCTGCATCGTTTGGG	TTCTGTCACTCTCTCTTTCCA
<i>TNF-α</i>	CAGAGGGAAGAGTCCCCAG	CCTTGGTCTGGTAGGAGACG
<i>TGF-β</i> <i>IL-1β</i> <i>IL-6</i>	GATGTCACCGGAGTTGTGCG CCACAGACCTTCCAGGAGAATG AGACAGCCACTCACCTCTTCAG	GCCGGTAGTGAACCCGTTGAT GTGCAGTTCAGTATCGTACAGG TTCTGCCAGTGCCTCTTTGCTG
<i>GAPDH</i>	GACAGTCAGCCGCATCTTCT	GCGCCCAATACGACCAAATC
<i>mIL-1β</i>	TGCCACCTTTTGACAGTGATG	TGTGTGCGAGATTTGA
<i>mIL-6</i> <i>mIFN-γ</i>	CCCCAATTTCCAATGCTCTCC CCAAGACTGTGATTGCGGGG	CGCACTAGGTTTGGCCGAGTA CTGGCCCGGAGTGTAGACAT
<i>mGAPDH</i>	CATCACTGCCACCCAGAAGACTG	ATGCCAGTGAGCTTCCCCTTCAG

**Table 2.** Primers sequences list.

### Statistical analysis

All experiments were performed at least in triplicate. Where data were normally distributed, the significance was determined using one-way ANOVA followed by a Holm-Sidak multiple comparisons test. The data were presented as the mean ± standard deviation. All statistical analyses were performed using GraphPad Prism software (version 8.0.2).

## Results

### Regional association between *ACP5* and allergy-related diseases risk

First, we investigated *ACP5*-associated variants and allergy-related disease risks. A family-based association test was performed to identify variants associated with any of four different types of allergy-related disease: allergic disease, asthma, atopic dermatitis, and allergic rhinitis. To exclude low quality information, the genotype data were quality controlled based on the following criteria: (1) samples were excluded if gender discrepancy, low call rate (<97%), excessive heterozygosity, and outliers of principle component analysis, (2) variants were excluded for low call rate (<95%), excessive Mendel errors, Hardy Weinberg equilibrium (HWE) failure ( $P < 10^{-6}$ ), and monomorphic frequency (minor allele frequency = 0). Among the associated variants, putative causal variants were selected based on the following two criteria and taken forward to experimental validation: nonsynonymous and  $p < 1 \times 10^{-3}$  for all allergic diseases. The underlying concept is that susceptibility to certain diseases should be linked with specific variants across the populations. In this study, we identified several candidate genes in a potentially susceptible genetic region, 11,687,195, on chromosome 19. Based on association results in the region, we propose *ACP5* as a top signaling gene for allergy-related diseases (Fig. 1B). To mimic *ACP5* SNPs, we established the *ACP5* knock-out BEAS-2B cell line using CRISPR/Cas9 editing and proliferation of *ACP5* knock-out BEAS-2B cell line was not significantly different from that of naïve BEAS-2B cell line (Fig. 1C, Supplementary Fig. 1). As a result, *ACP5* protein expression decreased significantly from 89.14% in naïve cells to 0.79% in *ACP5* KO cells as confirmed by flow cytometry (Fig. 1D).

### DEP increases cellular apoptosis and inflammation response in *ACP5* KO BEAS-2B cells via ROS

Next, we used an apoptosis assay to assess the DEP-induced viability of these *ACP5* KO cells. Incubation with 30 µg/mL or lower concentrations of DEP did not affect cell viability, but at 50 µg/mL and 100 µg/mL DEP induced cellular significant apoptosis and necrosis in both naïve and *ACP5* KO cells (Fig. 2A and B). Based on these results, a DEP concentration of 50 µg/mL was used in subsequent experiments. In a previous study, we confirmed that activation of the ROS/ERK/cFos signaling pathway is involved in DEP-induced therapeutic impairment of human Wharton's jelly-derived mesenchymal stem cells<sup>13</sup>. Because DEP-induced pathophysiology is largely due to ROS-mediated cellular apoptosis, we assessed induction of ROS in DEP-treated BEAS-2B cells using ROS-sensitive fluorophore 2',7'-dichlorofluorescein diacetate (DCFDA) staining. At a DEP concentration of 50 µg/mL, intracellular ROS increased significantly in *ACP5* KO cells (Fig. 2C). To determine whether DEP-

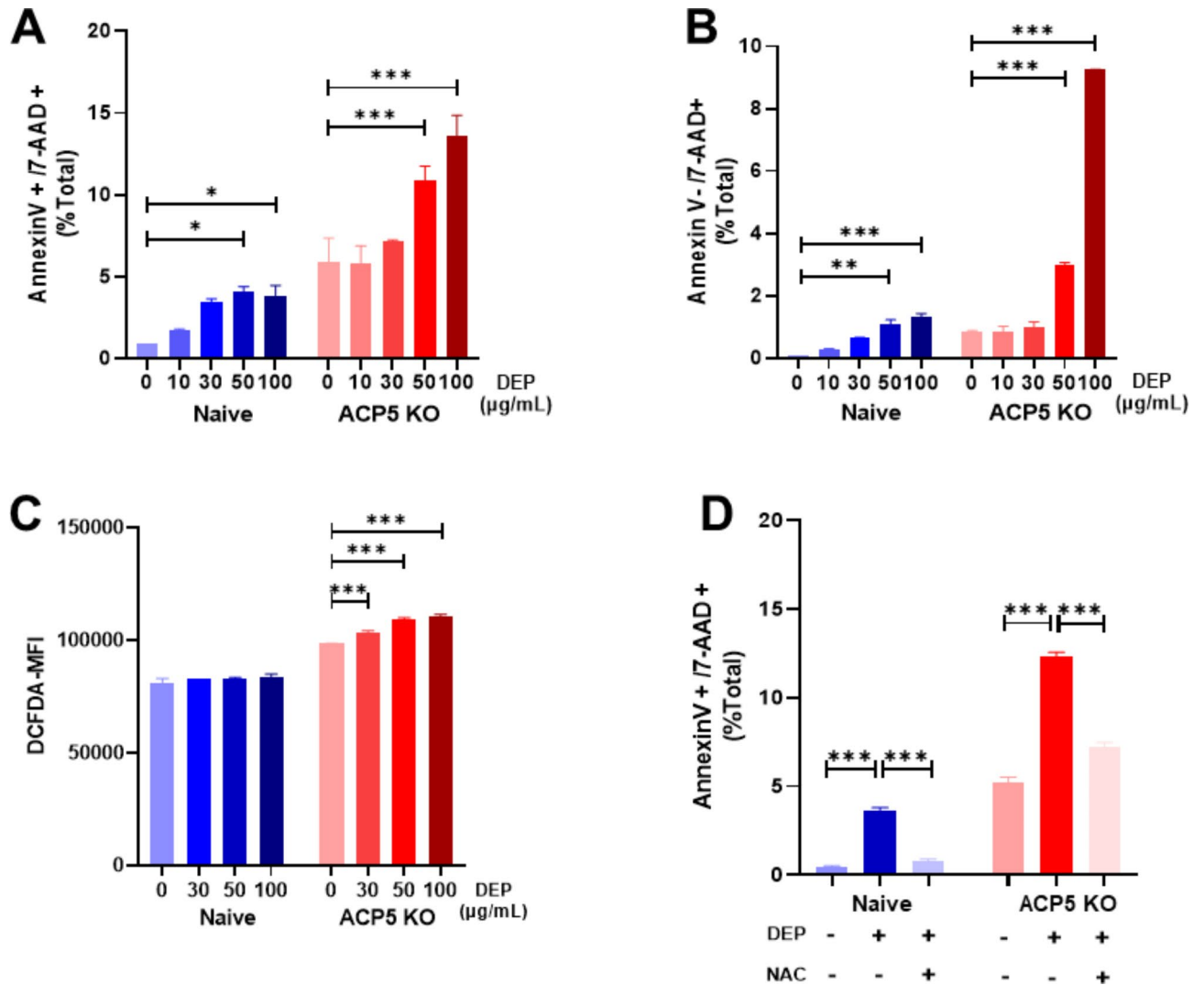


**Fig. 2.** DEP regulates apoptosis and ROS responses in *ACP5* KO BEAS-2B cells. (A, B) Naïve and *ACP5* KO BEAS-2B cells were treated with DEP (0–100 µg/mL) for 24 h. Apoptosis and necrosis rates were measured by labeling with Annexin-V-FITC and 7-AAD for flow cytometry analysis. Cells were stimulated with DEP (50 µg/mL) for 24 h. (C) Naïve and *ACP5* KO BEAS-2B cells were incubated with DEP at the indicated concentrations for 6 h. Intracellular ROS levels were measured using DCFDA and analyzed by flow cytometry. (D) Naïve and *ACP5* KO BEAS-2B cells were pretreated with 10 mM of NAC for 30 min and incubated with 50 µg/mL of DEP for 24 h. Apoptosis rates were measured by labeling with Annexin-V-FITC and 7-AAD for flow cytometry analysis. \* $p < 0.05$ , \*\* $p < 0.01$ , \*\*\* $p < 0.001$ .

induced ROS is implicated in the apoptosis properties of BEAS-2B cells, we performed a cell apoptosis assay in the presence of an ROS inhibitor, NAC (N-acetyl-L-cysteine). The cells were pretreated for 30 min with NAC and then treated with DEP for 24 h. DEP-induced apoptosis in *ACP5* KO cells was reversed by the ROS inhibitor (Fig. 2D). These data indicate that *ACP5* KO cells are susceptible to DEP-induced apoptosis through the activation of an ROS response.

#### DEP-treated *ACP5* KO BEAS-2B cells show AHR activation and pro-inflammatory responses

RNA sequencing was used to examine changes in the gene expression profile of DEP-treated *ACP5* KO BEAS-2B cells. Gene Ontology (GO) predicted activation of inflammation mediated by chemokine and cytokine signaling pathways in DEP-treated *ACP5* KO BEAS-2B cells (Fig. 3A). We therefore selected inflammation-related genes, and differential gene expression profiles were visualized with a hierarchical clustering heat map and a volcano plot. Clustering analyses revealed distinct patterns of differently expressed genes clustering in *ACP5* KO BEAS-2B cells with or without DEP exposure (Fig. 3B, Supplementary Fig. 2). To investigate the major contributor of inflammatory signaling in *ACP5* KO BEAS-2B cells, we analyzed the signaling networks associated with the activities of inflammatory genes using IPA. *CYP1A1*, *FOS*, and *NLRP3*, which are key regulators of inflammation signaling in DEP-treated *ACP5* KO cells, activate pro-inflammatory cytokines such as IL-6, IL1 $\beta$ , and CXCL2 (Fig. 3C). Because *CYP1A1* was determined to be a key regulator, we next confirmed the expression of genes

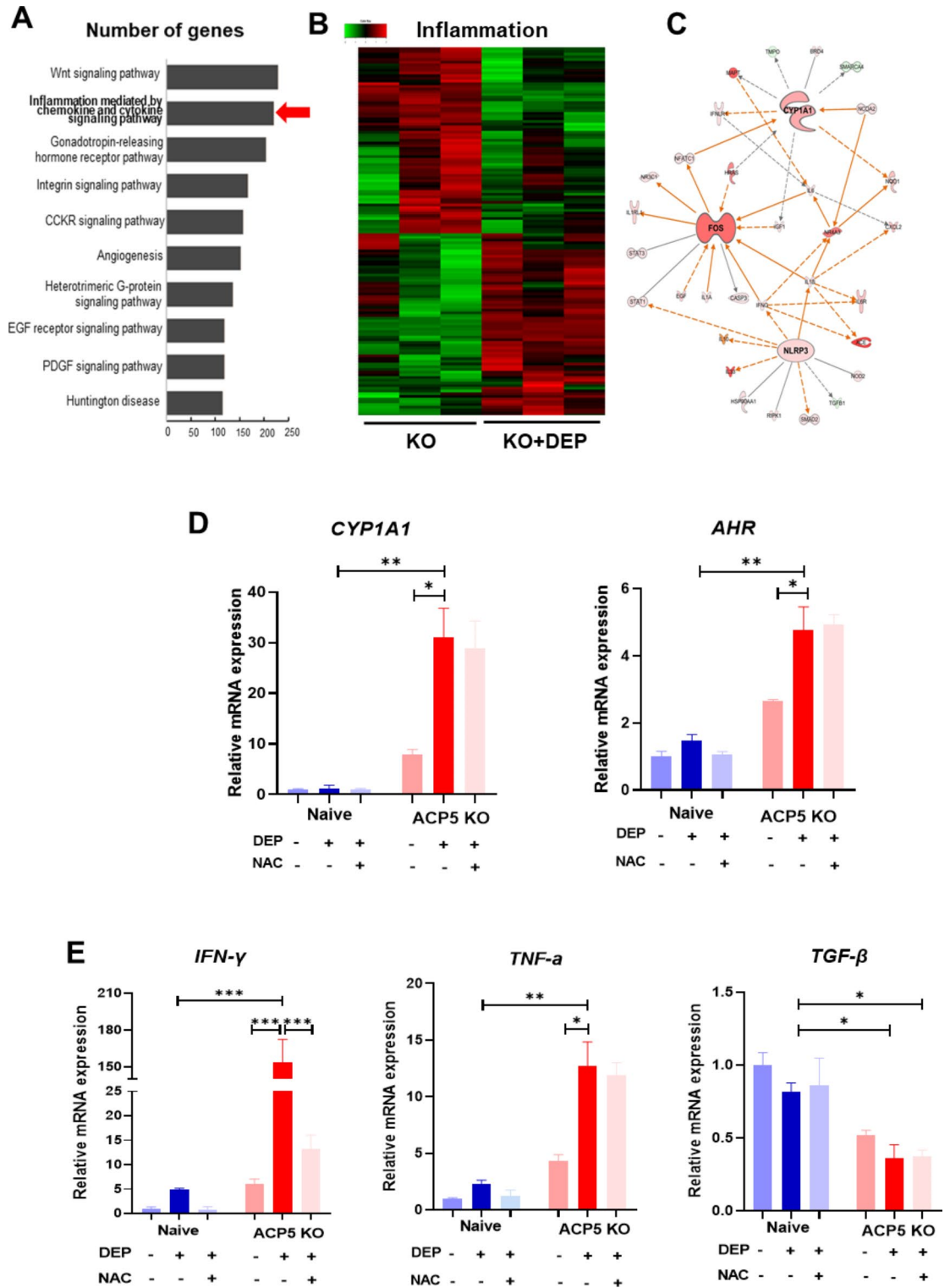


**Fig. 3.** DEP-treated BEAS-2B cells express ROS and pro-inflammatory responses. (A) Top-10 activated pathways predicted by GO in DEP-treated *ACP5* KO BEAS-2B cells compared with non-treated *ACP5* KO BEAS-2B cells. (B) Heat map of hierarchical clustering of DEG related to inflammation for *ACP5* KO BEAS-2B cells with or without DEP treatment ( $p < 0.05$ ). (C) Differentially expressed genes in DEP-treated *ACP5* KO BEAS-2B cells and non-treated *ACP5* KO BEAS-2B cells were investigated by IPA to assess the correlation network of various inflammation-related pathways and transcription factors. (D) Expression levels of ROS-related genes were determined by qRT-PCR and normalized to *GAPDH* expression. (E) Expression levels of inflammation-related genes were determined by qRT-PCR. \* $p < 0.05$ , \*\* $p < 0.01$ , \*\*\* $p < 0.001$ .

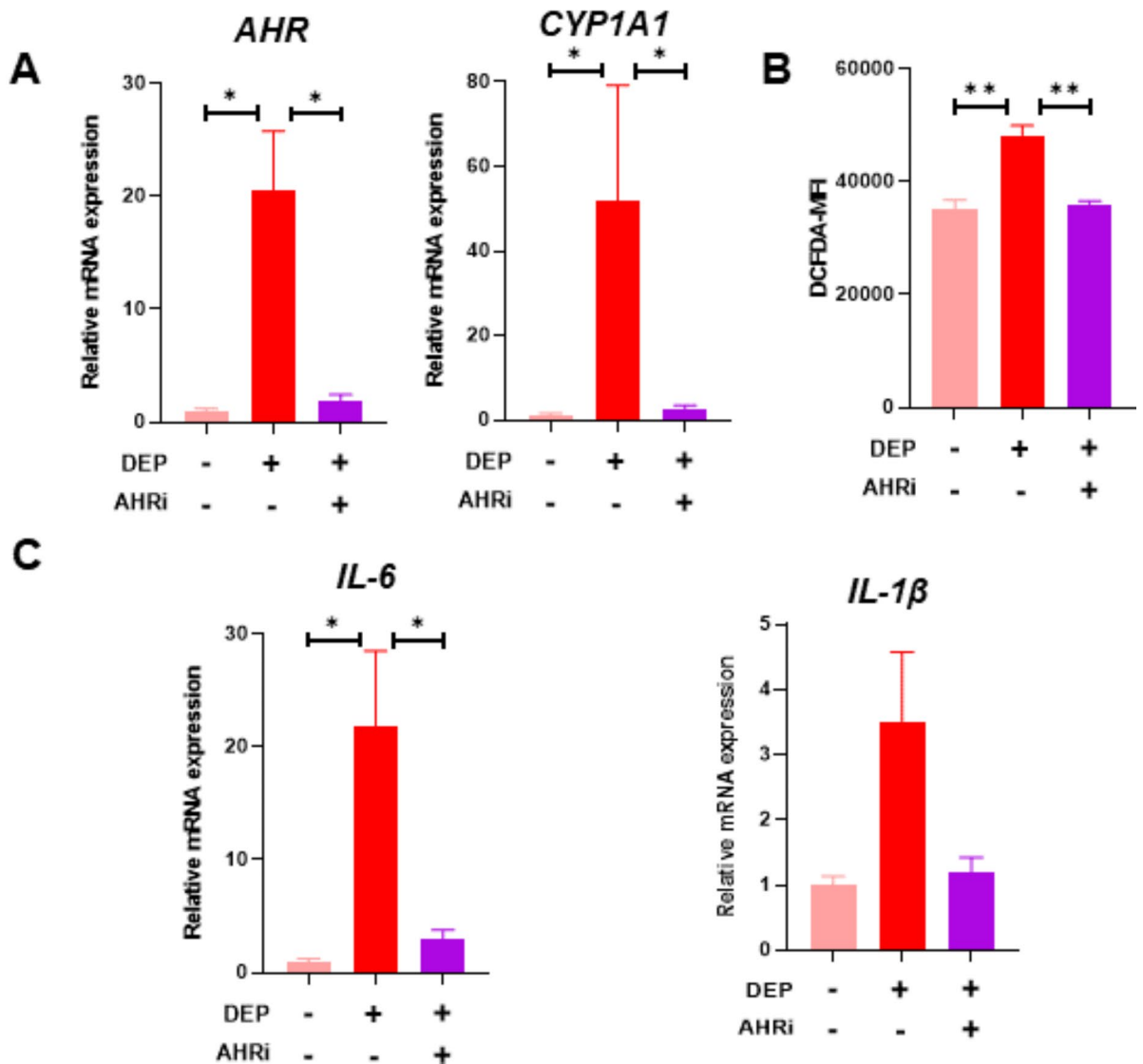


**Fig. 4.** Inhibition of AHR signaling ameliorated inflammation response in DEP-treated ACP5 KO BEAS-2B cells. **(A)** Expression levels of AHR and CYP1A1 after treatment with the AHR inhibitor BAY-218 as determined by qRT-PCR. **(B)** Intracellular ROS levels were measured using the ROS-sensitive DCFDA and analyzed by flow cytometry. **(C)** Expression levels of *IL-6* and *IL-1β* after treatment with 0.75 μM of AHR inhibitor BAY-218 were determined by qRT-PCR. Cells were pretreated for 30 min with the AHR inhibitor and stimulated with DEP (50 μg/mL) for 24 h. \* $p < 0.05$ , \*\* $p < 0.01$ , \*\*\* $p < 0.001$ .

up- and downstream of *CYP1A1*. Expression of CYP1A1 and AHR was significantly upregulated in ACP5 KO cells compared to naïve cells, and further upregulated upon DEP treatment (Fig. 3D). Expression levels of inflammation-related cytokines such as IFN-γ and TNF-α were also higher, but TGF-β expression was decreased in DEP-treated ACP5 KO cells (Fig. 3E). These results indicate that ACP5 KO BEAS-2B cells are sensitive to DEP-induced pro-inflammatory signaling specifically associated with the AHR-CYP1A1 axis.

#### DEP-treated ACP5 KO BEAS-2B induces ROS and a pro-inflammatory response through AHR signaling

We then investigated the regulatory role of AHR inhibition on the paracrine-mediated pro-inflammatory response. Pretreatment of an AHR inhibitor, BAY-218, significantly inhibited the activation of AHR and CYP1A1 in DEP-treated ACP5 KO BEAS-2B cells (Fig. 4A). The AHR inhibitor effectively blocked ROS responses (Fig. 4B) and inhibited the expression of pro-inflammatory cytokines such as IL-1β, IL-6 (Fig. 4C). These results suggest that AHR inhibition regulates ROS production, and pro-inflammatory signaling.

#### DEP-treated ACP5 KO BEAS-2B CM induces tissue damage in mice

To determine whether DEP-treated ACP5 KO BEAS-2B CM induces an inflammation response in mouse tissue, a concentrated (100×) CM was administered to mice (Fig. 5A). Mice in the DEP-treated ACP5 KO BEAS-2B CM

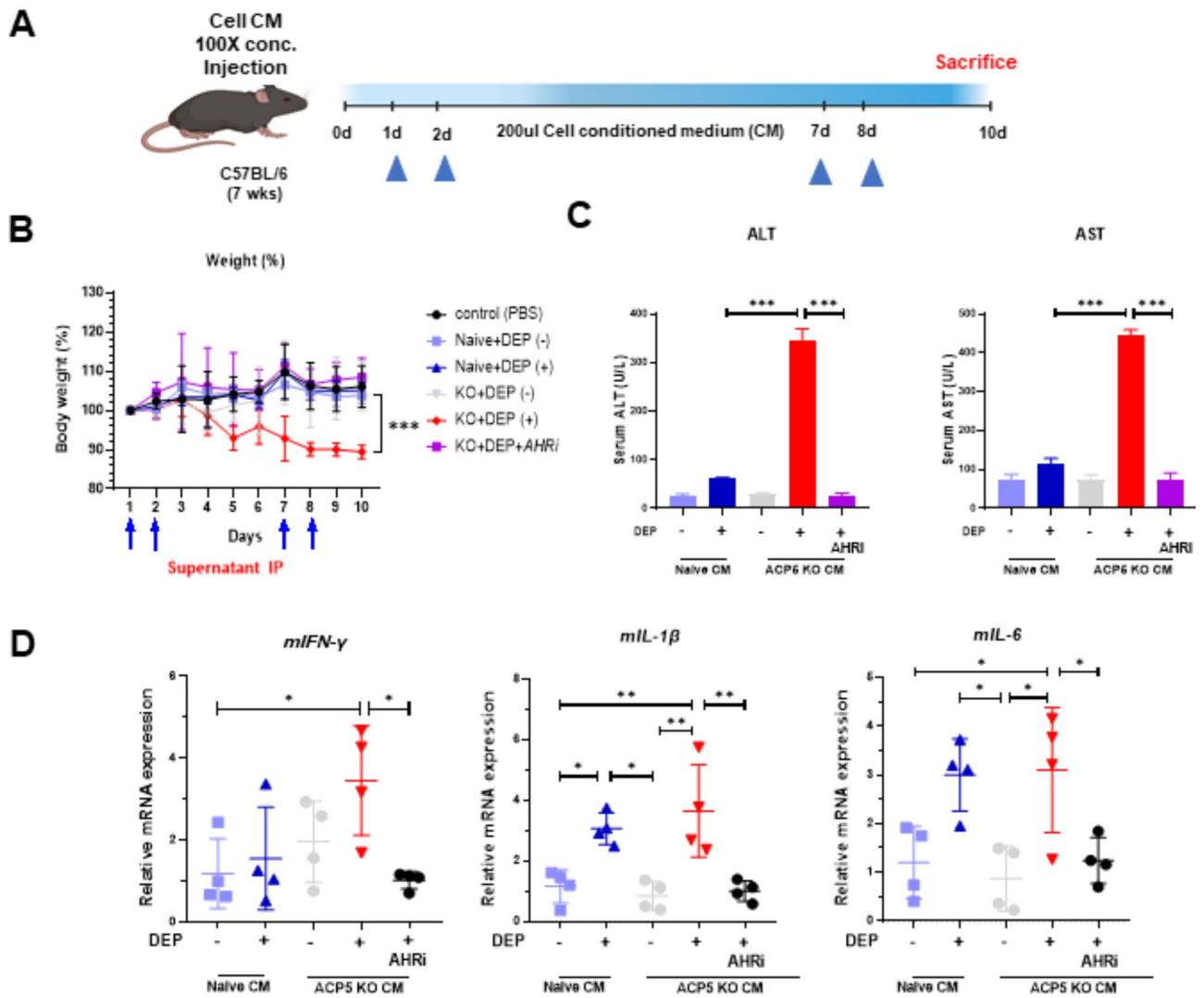


**Fig. 5.** DEP-treated ACP5 KO BEAS-2B CM induces liver tissue damages in mice. (A) A schematic of the in vivo experiment. Mice were sensitized on days 1, 2, 7, 8 by intraperitoneal injection of 200 µL of DEP-treated ACP5 KO BEAS-2B CM (100×) (B) The percentage of body weight change. (C) Serum ALT and AST levels. (D) DEP-treated ACP5 KO BEAS-2B CM-treated mice were sacrificed on day 10 and mRNA expression levels of inflammatory cytokines in liver tissues were analyzed by qRT-PCR. \* $p < 0.05$ , \*\* $p < 0.01$ , \*\*\* $p < 0.001$ .

group displayed continuous loss of body weight after CM injection (Fig. 5B). Serum ALT and AST levels were elevated significantly in the DEP-treated ACP5 KO BEAS-2B CM group; however, the AHR inhibitor treated groups showed low ALT and AST levels similar to those of the naïve groups (Fig. 5C). Expression levels of the pro-inflammatory cytokines mIFN- $\gamma$ , miL-1 $\beta$  and miL-6 were significantly increased in liver of members of the DEP-treated ACP5 KO BEAS-2B CM group, but downregulated in the AHR inhibitor group (Fig. 5D). These results indicate that DEP-treated ACP5 KO BEAS-2B CM induces cellular inflammation as well as tissue damage in mice.

## Discussion

The ACP5 protein is a mannose-rich glycoprotein that can be distinguished from other acid phosphatases because of its resistance to inhibition by tartrate. ACP5 has extensive pathophysiological functions depending on cell type and disease, and is involved in generations of ROS, osteoblast regulation, macrophage function, tumor progression and migration, and tissue fibrosis<sup>14</sup>. Although ACP5's pathophysiological roles have been extensively studied in the contexts of tumor progression and bone remodeling, its involvement in immune regulation, particularly in relation to environmental pollutants, remains largely unexplored. While this study focuses on bronchial epithelial cells, ACP5 has been implicated in broader immune regulation, particularly in T-cell responses. Prior research has shown that ACP5 deficient patients exhibit autoimmune phenotypes characterized by elevated type I interferon activity<sup>9</sup>, and ACP5-null mice macrophages exhibit increased levels of pro-inflammatory cytokines such as IL-1 $\beta$ , TNF- $\alpha$ , and IL-12<sup>8</sup>. These changes suggest that ACP5 may play a role

in shaping the immune balance between Th1 and Th2 responses, as well as regulatory T-cell (Treg) function. For instance, reduced TGF- $\beta$  expression in ACP5 KO cells could impair Treg differentiation, while elevated IFN- $\gamma$  levels may skew T-cell polarization toward a Th1 phenotype, contributing to inflammation and tissue damage. While these broader immune interactions were not directly addressed in our study, they provide an important avenue for future research to explore how ACP5 deficiency influences T-cell-mediated responses in allergic and autoimmune diseases.

Family-based association tests in 215 trios with allergy-related diseases revealed frequent missense mutations of ACP5 (Fig. 1A). In a previous study, Briggs et al. reported that an almost complete lack of ACP5 synthesis or secretion in patients with bi-allelic null mutations of ACP5<sup>9</sup>. Furthermore, homozygous or heterozygous missense mutations of ACP5 also act as null mutations, possibly through significant protein destabilization or impaired enzyme function due to interference with protein folding<sup>15</sup>. Because loss of ACP5 expression is closely related to immunogenic phenotype and elevated pro-inflammatory cytokines<sup>8,9</sup>, we investigated the capacity of knock-out ACP5 to further test the susceptibility to DEP exposure.

Loss of ACP5 in BEAS-2B cells increased susceptibility to DEP exposure, resulting in significantly elevated ROS levels and apoptosis (Fig. 2). We also found a significant increase of AHR expression in ACP5 KO BEAS-2B cells with elevated expressions of CYP1A1, IFN- $\gamma$ , and TNF- $\alpha$  (Fig. 3). Numerous studies have shown that CYP1A subfamily expression is induced by the activation of the AHR and AHR nuclear translocator (ARNT) as AHR/ARNT heterodimeric transcription factor translocates into the nucleus<sup>16</sup>. We confirmed that AHR inhibitors significantly decreased CYP1A1 and other pro-inflammatory factors, whereas NAC only inhibited pro-inflammatory cytokines, suggesting that DEP induced AHR-mediated CYP1A1-ROS signaling, which leads to significant inflammation. Our study provides evidence linking ACP5 deficiency to increased AHR expression and activation of the AHR-CYP1A1 inflammatory axis, though the precise upstream mechanisms remain unclear. Elevated ROS levels observed in DEP-treated ACP5 KO cells (Fig. 2C) suggest that ROS-mediated activation of AHR amplifies the inflammatory response through CYP1A1 transcription and downstream signaling. Additionally, the loss of ACP5 may disrupt TGF- $\beta$  signaling, as reduced TGF- $\beta$  expression in ACP5 KO cells aligns with previous studies demonstrating that ACP5 interacts intracellularly with TGF- $\beta$  receptor interacting protein-1 (TRIP-1), thereby activating TGF- $\beta$  receptor type 2 (TGF $\beta$ R2) and Smad2/3 signaling<sup>17</sup> indicating that TGF- $\beta$  negatively regulates AHR expression. Further studies are needed to validate these mechanisms, including investigating transcription factor interactions at the AHR promoter and the role of ROS scavengers. BEAS-2b is a non-tumorigenic and non-invasive immortalized human bronchial epithelial cell line associated with the transforming adenovirus SV40 and it behaves in a manner similar to that of normal lung cells<sup>18</sup>. Because transcriptome analysis of DEP-exposed ACP5 KO BEAS-2b cells found significantly upregulated inflammation mediated by chemokines and the cytokine signaling pathway, we assumed that DEP-exposed ACP5-mutated lung cells could also affect the physiological processes of neighboring cells through an inflammatory secretome. BEAS-2b cells can trigger an immunological response, including pro-inflammatory signals through the secretion of proteins when exposed to particulate air pollutants<sup>19,20</sup>. We administrated 100 $\times$ -concentrated cell-cultured supernatants from DEP-exposed wild-type or ACP5 KO BEAS-2b cells to C57BL/6 mice. Supernatants from the ACP5 KO cells induced systemic inflammation. However, co-treatment of AHR-inhibitor inhibited the inflammatory response, suggesting AHR signal plays an important role in the immunological response.

Inhibition of AHR signaling using BAY-218 effectively reduced DEP-induced ROS production, pro-inflammatory cytokine expression, and tissue damage in vitro and in vivo, highlighting the AHR-CYP1A1 axis as a promising therapeutic target, particularly for individuals with ACP5 mutations. However, the broader implications of targeting this axis require caution. AHR plays a dual role, mediating detoxification while potentially generating reactive intermediates that contribute to oxidative stress and carcinogenesis<sup>21,22</sup>. Prolonged or systemic AHR inhibition may disrupt homeostasis, leading to unmetabolized xenobiotics and adverse effects. Therefore, while short-term AHR inhibition shows potential, further studies are essential to ensure the safety and efficacy of AHR-targeted therapies and to fully elucidate ACP5-AHR interactions in diverse contexts.

In summary, the use of CRISPR/Cas9-mediated ACP5 KO to mimic frequently found ACP5 missense mutations resulted in increased apoptosis and an ROS damage response upon exposure of BEAS-2B cells to DEP. Transcriptome analysis revealed a significantly increased inflammation- and apoptosis-signaling pathway, and we confirmed that activation of the AHR-CYP1A1 axis followed by pro-inflammatory signaling appears to be a prominent mechanism underlying detrimental effects. Finally, we demonstrated that AHR inhibition in DEP-exposed ACP5 KO BEAS-2B cells effectively prevented inflammation-induced damage both in vitro and in vivo, suggesting that targeting the AHR-CYP1A1 axis has therapeutic applications in individuals suffering from DEP-induced toxicity, particularly patients with ACP5 mutations.

## Data availability

RNA-seq data supporting the results of this study have been deposited in the NCBI GEO database under accession number GSE278107 (<https://www.ncbi.nlm.nih.gov/geo/query/acc.cgi?acc=GSE278107>).

Received: 19 June 2024; Accepted: 23 December 2024

Published online: 14 March 2025

## References

- Xia, N. & Li, H. Loneliness, social isolation, and Cardiovascular Health. *Antioxid. Redox Signal.* **28**(9), 837–851 (2018).
- Yu, C. P. & Xu, G. B. Predictive models for deposition of inhaled diesel exhaust particles in humans and laboratory species. *Res. Rep. Health Eff. Inst.*, **1987**(10), 3–22 (1987).
- Barouki, R. et al. The aryl hydrocarbon receptor system. *Drug Metabol Drug Interact.* **27**(1), 3–8 (2012).

4. Esser, C. & Rannug, A. The aryl hydrocarbon receptor in barrier organ physiology, immunology, and toxicology. *Pharmacol. Rev.* **67**(2), 259–279 (2015).
5. Quintana, F. J. et al. Control of T(reg) and T(H)17 cell differentiation by the aryl hydrocarbon receptor. *Nature* **453**(7191), 65–71 (2008).
6. van Eeden, S. F. et al. Cytokines involved in the systemic inflammatory response induced by exposure to particulate matter air pollutants (PM<sub>10</sub>). *Am. J. Respir. Crit. Care Med.* **164**(5), 826–830 (2001).
7. Oddie, G. W. et al. Structure, function, and regulation of tartrate-resistant acid phosphatase. *Bone* **27**(5), 575–584 (2000).
8. Bune, A. J. et al. Mice lacking tartrate-resistant acid phosphatase (acp 5) have disordered macrophage inflammatory responses and reduced clearance of the pathogen, *Staphylococcus aureus*. *Immunology* **102**(1), 103–113 (2001).
9. Briggs, T. A. et al. Tartrate-resistant acid phosphatase deficiency causes a bone dysplasia with autoimmunity and a type I interferon expression signature. *Nat. Genet.* **43**(2), 127–131 (2011).
10. Laird, N. M., Horvath, S. & Xu, X. Implementing a unified approach to family-based tests of association. *Genet. Epidemiol.* **19**(Suppl 1), S36–42 (2000).
11. Pruim, R. J. et al. LocusZoom: regional visualization of genome-wide association scan results. *Bioinformatics* **26**(18), 2336–2337 (2010).
12. Park, H. S. et al. Cigarette smoke impairs the hematopoietic supportive property of mesenchymal stem cells via the production of reactive oxygen species and NLRP3 activation. *Stem Cell Res. Ther.* **15**(1), 145 (2024).
13. Park, H. S. et al. Diesel Exhaust particles impair therapeutic effect of Human Wharton's jelly-derived mesenchymal stem cells against experimental colitis through ROS/ERK/cFos signaling pathway. *Int. J. Stem Cells.* **15**(2), 203–216 (2022).
14. Ren, X. et al. ACP5: its structure, distribution, regulation and novel functions. *Anticancer Agents Med. Chem.* **18**(8), 1082–1090 (2018).
15. Ramesh, J. et al. Characterisation of ACP5 missense mutations encoding tartrate-resistant acid phosphatase associated with spondyloenchondrodysplasia. *PLoS One.* **15**(3), e0230052 (2020).
16. Ma, Q. Induction of CYP1A1. The AhR/DRE paradigm: transcription, receptor regulation, and expanding biological roles. *Curr. Drug Metab.* **2**(2), 149–164 (2001).
17. Reithmeier, A. et al. Tartrate-resistant acid phosphatase (TRAP/ACP5) promotes metastasis-related properties via TGFβ<sub>2</sub>/TβR and CD44 in MDA-MB-231 breast cancer cells. *BMC Cancer.* **17**(1), 650 (2017).
18. Reddel, R. R. et al. Transformation of human bronchial epithelial cells by infection with SV40 or adenovirus-12 SV40 hybrid virus, or transfection via strontium phosphate coprecipitation with a plasmid containing SV40 early region genes. *Cancer Res.* **48**(7), 1904–1909 (1988).
19. Veranth, J. M. et al. Inflammatory cytokines and cell death in BEAS-2B lung cells treated with soil dust, lipopolysaccharide, and surface-modified particles. *Toxicol. Sci.* **82**(1), 88–96 (2004).
20. Fuentes-Mattei, E. et al. Use of human bronchial epithelial cells (BEAS-2B) to study immunological markers resulting from exposure to PM<sub>2.5</sub> organic extract from Puerto Rico. *Toxicol. Appl. Pharmacol.* **243**(3), 381–389 (2010).
21. Fan, Y. et al. The Aryl Hydrocarbon Receptor Functions as a tumor suppressor of liver carcinogenesis. *Cancer Res.* **70**(1), 212–220 (2010).
22. Feng, S., Cao, Z. & Wang, X. Role of aryl hydrocarbon receptor in cancer. *Biochimica et Biophysica Acta (BBA) - Reviews on Cancer* **1836**(2), 197–210 (2013).

## Acknowledgements

This work was supported by the Research Grant from Seoul National University (0525-20220151), and Korea National Institute of Health (KNIH) (2020-NG-010-02, 2015-NI-67002-00) and multidisciplinary research grant-in-aid from the Seoul Metropolitan Government Seoul National University (SMG-SNU) Boramae Medical Center (04-2023-00) & SNU, Bio-MAX Institute.

## Author contributions

Conceptualization – H.J.L. and K.-R.Y.; Methodology – A.Y., H.B.A., D.Y., K.-S.P., H.M.Y., H.-S.K., K.-S.K., M.-K.O.; Investigation – A.Y., H.B.A., D.Y., H.-R.H., D.-H.C., U.C., H.S.P., J.H.P, M.H.H., J.-Y.H., K.C.; Writing – A.Y., D.Y., H.B.A., H.J.L., K.-R.Y.; Funding acquisition – H.-J.L., K.-R.Y.; Supervision – H.-J.L. and K.-R.Y. All authors have read and agreed to the published version of the manuscript.

## Declarations

### Competing interests

The authors declare no competing interests.

## Additional information

**Supplementary Information** The online version contains supplementary material available at <https://doi.org/10.1038/s41598-024-84280-9>.

**Correspondence** and requests for materials should be addressed to K.-R.Y.

**Reprints and permissions information** is available at [www.nature.com/reprints](http://www.nature.com/reprints).

**Publisher's note** Springer Nature remains neutral with regard to jurisdictional claims in published maps and institutional affiliations.

**Open Access** This article is licensed under a Creative Commons Attribution-NonCommercial-NoDerivatives 4.0 International License, which permits any non-commercial use, sharing, distribution and reproduction in any medium or format, as long as you give appropriate credit to the original author(s) and the source, provide a link to the Creative Commons licence, and indicate if you modified the licensed material. You do not have permission under this licence to share adapted material derived from this article or parts of it. The images or other third party material in this article are included in the article's Creative Commons licence, unless indicated otherwise in a credit line to the material. If material is not included in the article's Creative Commons licence and your intended use is not permitted by statutory regulation or exceeds the permitted use, you will need to obtain permission directly from the copyright holder. To view a copy of this licence, visit <http://creativecommons.org/licenses/by-nc-nd/4.0/>.

© The Author(s) 2025